Polymerized High Internal Phase Emulsions Containing a Porogen: Specific Surface Area and Sorption

Anatoly Y. Sergienko,[1] Huwen Tai,[1] Moshe Narkis,[2] Michael S. Silverstein[1]

[1]Department of Materials Engineering and the Grand Water Research Institute, Technion–Israel Institute of Technology, Haifa, 32000, Israel
[2]Department of Chemical Engineering and the Grand Water Research Institute, Technion–Israel Institute of Technology, Haifa, 32000, Israel

ABSTRACT: Highly porous, open-cell polymers [poly(HIPE)] were prepared by polymerizing the monomers in the continuous phase ($\sim$ 10%) of high internal phase emulsions (HIPE). This paper discusses using poly(HIPE) to remove bromoform from an aqueous solution through sorption, a combination of adsorption and absorption. The crosslinked polystyrene (xPS) and crosslinked poly(ethylhexyl acrylate) (xPEHA) had cell diameters from 1.5 to 15 μm, intercellular pore diameters from 0.3 to 1.5 μm, and densities of about 0.10 g/cc. The specific surface area of the glassy xPS increased from 7.9 to 28.8 m^2/g on extraction in methanol, most likely due to crazing. The use of a toluene porogen in the xPS (xPS-T) reduced the density to 0.05 g/cc and yielded a rough surface with nanoscale porosity and a specific surface area of 132 m^2/g. xPS and xPEHA, with very different molecular structures but with similar specific surface areas, exhibited similar sorption behavior. Extraction produced increases in the xPS and xPS-T sorption plateaus and sorption capacities. For larger specific surface areas, the sorption at low concentrations was relatively independent of concentration, indicating a case of adsorption with the sites occupied. For all the other cases, absorption seems to dominate and sorption is more strongly dependent upon concentration. © 2004 Wiley Periodicals, Inc. J Appl Polym Sci 94: 2233–2239, 2004

Key words: emulsion polymerization; adsorption; polystyrene; porogen; specific surface area

INTRODUCTION

Potable water undergoes disinfection using oxidants such as chlorine, chlorine dioxide, chloroamines, and ozone. Traces of the disinfectant remain in the water since pathogens may subsequently enter the system. Unfortunately, the disinfectant may also react with organic materials in the water and form disinfection byproducts (DBP) that may be carcinogenic. Trihalomethanes (THMs) are among the principal DBPs of concern with respect to their effects on health.[1] The technologies available for removing DBPs from water include granular activated carbon (GAC) adsorption, biological degradation, distillation, air stripping, ozone oxidation, reverse osmosis, and pervaporation.[2–8] Another option for removing DBP from water may be a combination of adsorption and absorption, hereafter referred to as sorption, by porous polymeric absorbents contained in a packed column.[9–13]

Synthetic polymeric absorbent resins are applicable for specific absorption cases and lend themselves adequately to chemical regeneration and absorbate re-

covery.[9] Pilot studies have shown that polymeric resins can remove THMs and other chlorinated organics more effectively and for longer periods of time than GAC.[14] Some polymers have exhibited longer breakthrough times and higher operating capacities than GAC at the same effluent flow rate.[15] There are two families of commercial nonionic polymeric absorbent resins. One is based on crosslinked polystyrene and another on crosslinked polymethacrylate.[16] Styrene–divinylbenzene resins have received much attention as absorbents for removing pesticides and related compounds and for removing chlorinated compounds.[17] The crosslinking is used to make the resins more durable.[9] The terminology for polymeric materials is not always exact, since surface adsorption is followed by volume absorption within the polymer. The term sorption will be used to describe these phenomena.

A high internal phase emulsion (HIPE) has a continuous minor organic phase (less than 25%) within which is dispersed the major aqueous phase (more than 75%). When the organic phase consists of a monomer and the aqueous phase includes an initiator, a polymerization reaction can take place within the HIPE, yielding a polymerized HIPE [poly(HIPE)].[18–22] Porous polymers with cell dimensions on the micrometer scale are produced by removing the aqueous

phase through drying. The volume fraction of solid in poly(HIPE) can be as low as 0.03 and the cells are interconnected through intercellular pores. The bulk density is typically less than 0.15 g/cm^3 and the cell size ranges between 5 and 100 μm. The structure and properties of the poly(HIPE) can be varied through the addition of a crosslinking comonomer or a porogen to the organic phase.[23,24] Several applications of poly-(HIPE) have been examined and poly(HIPE) monoliths have exhibited good flow properties in column testing.[25–27] Recent studies have shown that the structure and properties of poly(HIPE) can be modified significantly through the formation of interpenetrating polymer networks (IPNs) or through the formation of organic–inorganic hybrid networks.[28–31]

This paper describes the removal of a typical THM from water using various poly(HIPE). The poly(HIPE) investigated were based on different polymers and were modified using a porogen. The relationships between the nature of the poly(HIPE), the specific surface area, and the sorption were explored.

EXPERIMENTAL

Materials

The monomers used for poly(HIPE) synthesis were styrene (S, Fluka Chemie) and 2-ethylhexyl acrylate (EHA, Aldrich). The poly(HIPE) were crosslinked by adding divinylbenzene containing 20% ethylstyrene (DVB, Riedel-de-Haen) as a comonomer. The monomers were used as received. The porogen added to the styrene was toluene (T, Frutarom, Israel). The emulsifier for the crosslinked polystyrene (xPS) poly(HIPE) was sorbitan monooleate (SMO, Span 80, Fluka Chemie) and the emulsifier for the crosslinked poly(2-ethylhexyl acrylate) (xPEHA) poly(HIPE) was sorbitan monolaurate (SML, Span 20, Fluka Chemie). SML was used for the HIPE containing EHA since it enhanced the stability of the HIPE during polymerization. The same amount of surfactant was used in the preparation of all poly(HIPE). The water soluble initiator was potassium persulfate (K$_2$S$_2$O$_8$, Riedel-de-Haen). The HIPE stabilizer was calcium chloride hydrate (CaCl$_2$·2H$_2$O, A.C.S., Israel). The haloorganic used as a contaminant was bromoform (BF, tribromomethane, Fluka Chemie).

Poly(HIPE) synthesis

The poly(HIPE) recipes for xPS, xPS containing toluene (xPS-T), and xPEHA are listed in Table I. Higher DVB contents were used for xPS-T and xPEHA poly-(HIPE) to prevent their collapse during polymerization. The poly(HIPE) synthesis procedure was described in detail elsewhere.[28,29] Briefly, a HIPE was formed by adding the aqueous phase (water, initiator

TABLE I
Poly(HIPE) Recipes

		xPS (g)	xPS-T (g)	xPEHA (g)
Organic phase	Monomer	9 (S)	4 (S)	8 (EHA)
	DVB	1	2	2
	Toluene	0	5	0
Aqueous phase	Water	90	90	90
	Initiator	0.2	0.2	0.2
	Stabilizer	0.5	0.5	0.5

and stabilizer, about 90% of the total volume) dropwise to the organic phase (monomers and emulsifier, about 10% of the total volume). The resulting HIPE was placed in an oven at 65°C for 18 h for polymerization. The poly(HIPE) was dried in a vacuum oven at 60°C for about 2 days until a constant weight was achieved. The relatively rapid drying reflects the open-cell structure of the poly(HIPE). The poly(HIPE) were then placed in a Soxhlet extraction apparatus. The extraction procedure was 24 h in water followed by 24 h in methanol. The poly(HIPE) were then dried in a convection oven at 60°C for 12 h. The sample names are modified to distinguish between a poly-(HIPE) before extraction (i.e., xPS-BE) and a poly-(HIPE) after extraction (i.e., xPS-AE) whenever necessary.

Poly(HIPE) characterization

The poly(HIPE) density was determined by measuring the mass and volume of a specimen. The poly-(HIPE) structure was investigated using high resolution scanning electron microscopy (HRSEM) of cryogenic fracture surfaces (LEO 982, Zeiss). The samples were usually not coated and were viewed using accelerating voltages from 1 to 3 kV. A thin gold coating was applied to view the cell wall structure at especially high magnifications. The specific surface area of the poly(HIPE) was determined by the single-point BET (Brunauer, Emmett, Teller) method with nitrogen adsorption–desorption at 77K (Flowsorb II, Micromeritics).

Sorption: rate studies

Solutions of BF in deionized water were prepared using a gas chromatograph syringe to precisely measure BF volume. The solution was covered tightly during mixing to prevent evaporation. The BF concentration in the solution phase was determined using UV spectroscopy at a wavelength of 220 nm (UV-2, Unicam). The calibration curve was linear for concentrations between 2.5 and 375 mg/L.

Rate studies involved determining the amount of bromoform sorbed as a function of time using sorption

rate experiments. Poly(HIPE) cubes (~ 0.15 g) were placed in flasks containing 40 mL of a 150 mg/L BF aqueous solution, one per flask, and held beneath the surface using a wire screen. The flasks were closed tightly and agitated continuously during the experiment. At predetermined times a single flask was withdrawn from the set and the concentration of BF in the solution was determined using UV spectrometry. The flask that was withdrawn was not used further. The amount of BF sorbed was calculated from the difference between the initial concentration and the concentration at the time the flask was withdrawn.

Sorption: equilibrium studies

Equilibrium studies were conducted using a conventional bottle-point technique. A 300 mg/L BF solution was prepared and then diluted to different concentrations. Poly(HIPE) cubes (~ 0.15 g) were placed in flasks containing 40 mL of a BF solution, one per flask, and held beneath the surface using a wire screen. The flasks were closed tightly and agitated continuously until an equilibrium was achieved. The equilibration time used, based on the rate studies, was 96 h. The concentration of BF in the solution was then determined using UV spectrometry. The amount of BF sorbed was calculated from the difference between the initial concentration and the equilibrium concentration.

RESULTS AND DISCUSSION

Poly(HIPE) structure

The xPS poly(HIPE) has an open-cell morphology and intercellular pores within the cell walls, as seen in Figure 1. The cells are 3–10 μm in diameter and the intercellular pores are 0.4–1.5 μm in diameter. The intercellular pores are ellipsoidal, bordering on trapezoidal, with angular cusps instead of rounded corners. The xPS cell walls appear smooth and uniform at high magnifications [Fig. 1(b)]. The effects of adding toluene to the styrene can be seen by comparing the poly(HIPE) structure for xPS-T in Figure 2 with that of xPS in Figure 1. The xPS-T poly(HIPE) has a cell size and an intercellular pore size similar to those of xPS, but the cells are more spherical in shape and the intercellular pores are more circular. The xPS-T cell walls are considerably rougher than those of xPS. At high magnification [Fig. 2(b) and (c)] it can be seen that this roughness is actually a nanoscale porosity throughout the walls. The three dimensional nature of the poly(HIPE) structure can be seen in Figure 2(b), where porous cell walls are clearly visible behind the intercellular pores. The nanoscale porosity in the walls is reflected in the 44% decrease in density, from 0.09 g/cc for xPS-AE to 0.05 g/cc for xPS-T-AE (Table II).
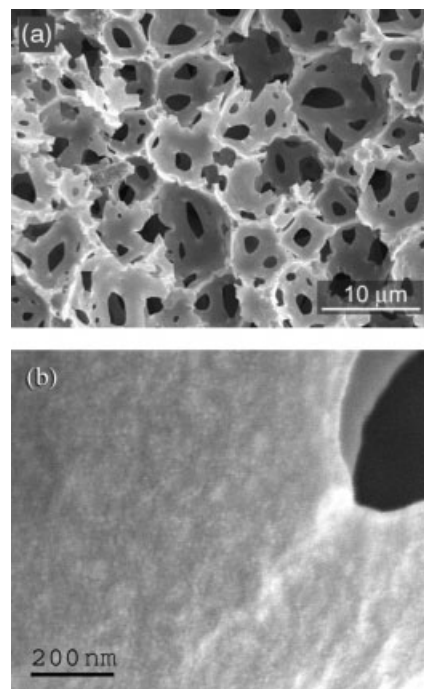

Figure 1 SEM micrographs of xPS poly(HIPE).

This reduction in density reflects the reduction in the HIPE monomer content.

The xPEHA poly(HIPE) has a density of 0.11 g/cc (Table II) and a somewhat different structure. The cells in the xPEHA poly(HIPE) (Fig. 3) are more circular in shape than those in the xPS poly(HIPE). There is a significantly wider, almost bimodal, distribution of xPEHA cell diameters. The average diameter of the smaller cells is 1.5 μm and the average diameter of the larger cells is 15 μm. The xPEHA poly(HIPE) also exhibits a relatively high density of intercellular pores and relatively small pore diameters, ranging from 0.3 to 1 μm. The differences between xPEHA and xPS in density, cell size, cell size distribution, intercellular pore size, and intercellular pore density have been associated with the different emulsifiers used.[30] SMO, used for the styrene HIPE, is a low viscosity emulsifier with a low hydrophilic–lypophilic balance (HLB), while SML, used for the EHA HIPE, is a high viscosity, high HLB emulsifier. There were, therefore, significant differences in interfacial tension and in viscosity between the HIPE containing styrene and SMO and the HIPE containing EHA and SML. The EHA HIPE exhibited a very high viscosity and was difficult to mix using mechanical stirring. The differences in HIPE interfacial tension and viscosity produced the differences in poly(HIPE) density and cellular structure.[30]

Specific surface area

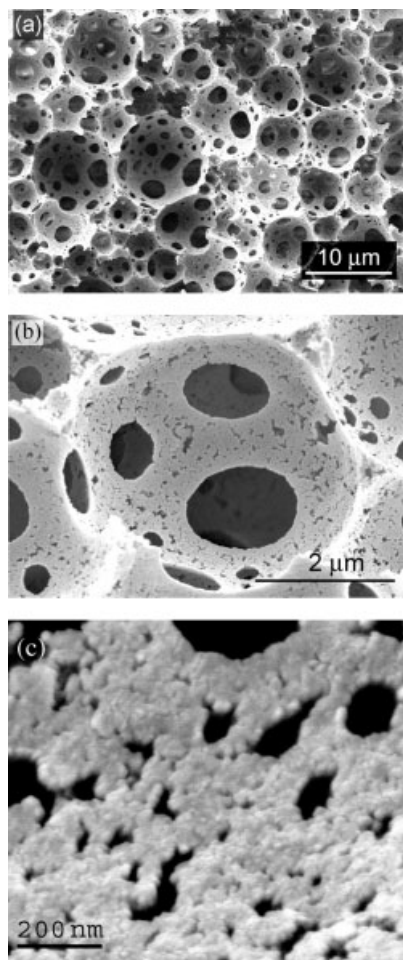The specific surface areas of the different poly(HIPE), before and after extraction, are listed in Table II. The

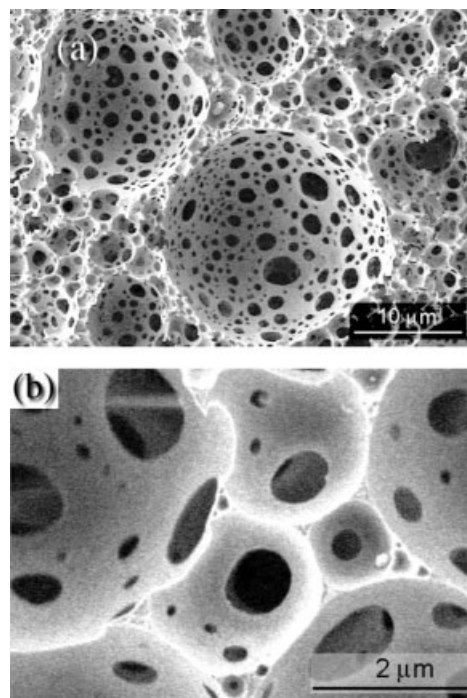**Figure 2** SEM micrographs of xPS-T poly(HIPE).

Figure 3 SEM micrographs of xPEHA poly(HIPE).

ing. In contrast, xPEHA exhibited a slight decrease in specific surface area following extraction. xPEHA is above its T_g of $-40°C$ during extraction in methanol and, therefore, is not prone to crazing.[32] Extraction of xPS-T yielded a specific surface area of 132 m²/g, an extraordinary 17-fold increase in specific surface area, reflecting the rough surface with nanoscale porosity in Figure 2(c).

Sorption: rate studies

The BF sorption by xPS and xPEHA from a 150 mg/L aqueous solution is seen in Figure 4, for both before and after extraction. A sorption plateau was reached after less than 20 h for all the poly(HIPE) studied. xPS-BE and xPEHA-BE, which have very different molecular struc-

specific surface areas of the as-synthesized poly(HIPE) (before extraction) ranged from 7.5 to 7.9 m²/g. xPS exhibited a significant increase in specific surface area following extraction, from 7.9 to 28.8 m²/g. This increase in specific surface area is believed to be produced by crazing in the glassy xPS. xPS is below its glass transition temperature (T_g) of 106°C during extraction in methanol and is, therefore, prone to crazing.

TABLE II
Poly(HIPE) Properties

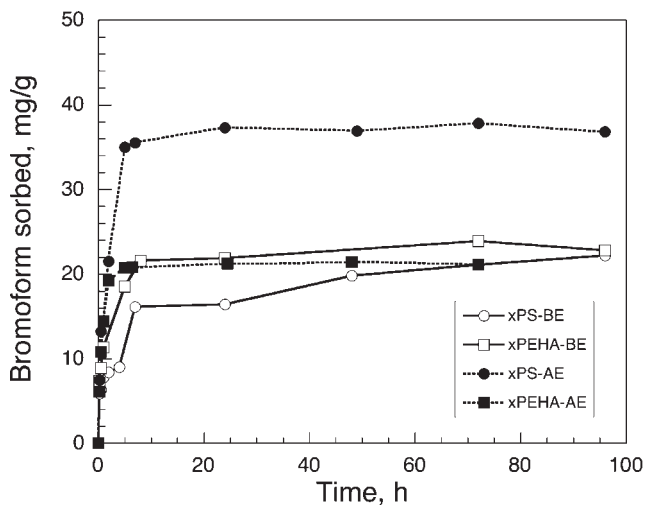|		Density (g/cc)	Specific surface area (m²/g)	K (mg/g)(L/mg)$^{1/n}$	$1/n$
xPS	BE	0.11	7.9	0.0066	1.86
	AE	0.09	28.5	0.330	1.29
xPEHA	BE	0.13	7.9	0.0062	1.86
	AE	0.11	7.0	0.103	1.28
xPS-T	BE	0.08	7.5	0.103	1.30
	AE	0.05	132	3.96[a]	0.74[a]
				26.1[b]	0.23[b]

[a] Higher C_e.
[b] Lower C_e.

Figure 4 Sorption from 150 mg/L BF solution for xPS and xPEHA, before and after extraction.

tures, exhibited similar BF sorption behavior. The sorption thus seems to be more strongly influenced by their similar specific surface areas than by their different molecular structures. Extraction yields an increase in specific surface area and in sorption for xPS while extraction yields a decrease in specific surface area and a decrease in sorption for xPEHA.

The influence of extraction on BF sorption by xPS and xPS-T from a 150 mg/L aqueous solution is seen in Figure 5. Both xPS-BE and xPS-T-BE exhibited relatively limited BF sorption, reflecting their relativley small specific surface areas. Extraction yields a significant increase in specific surface area and in sorption for xPS and xPS-T. Here again, the change in sorption is consistent with the change in specific surface area. The variation of the maximum in BF sorption for xPS and xPS-T, taken from the plateaus in Figure 5, with the specific surface
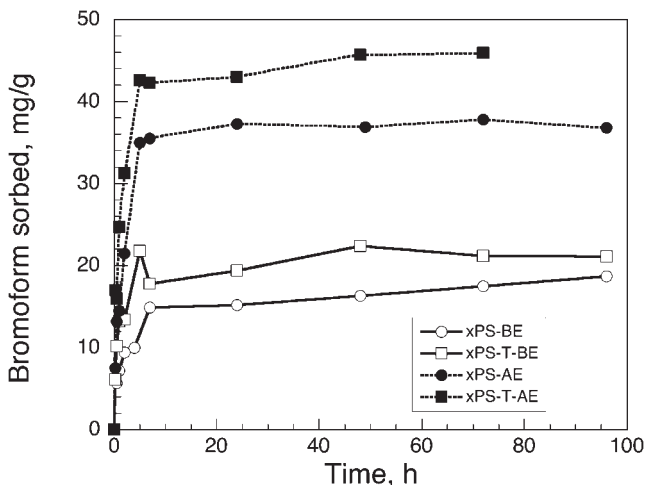
area (A_s) is plotted in Figure 6(a) using log–log axes. The slope of the straight line in Figure 6(a), representing the log–log dependence of the BF sorption plateaus on the specific surface area, is 0.15. The relatively small slope indicates that the BF sorption plateau is not strongly dependent on the specific surface area for the set of sorption conditions studied.

Sorption: equilibrium studies

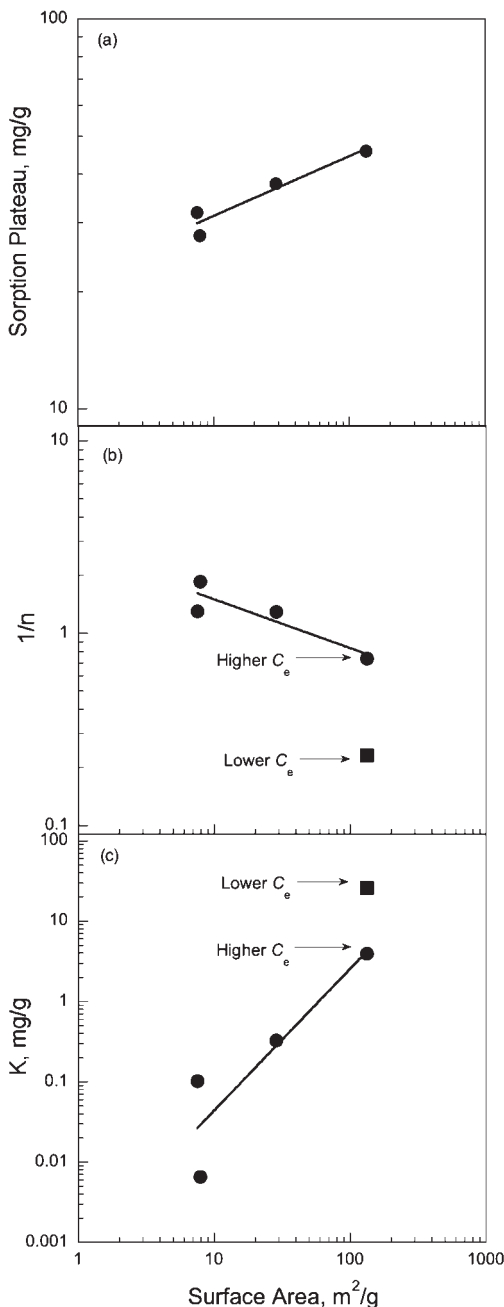Freundlich described the behavior of adsorption isotherms using Equations (1) and (2).

Figure 6 Sorption parameters as a function of specific surface area for xPS and xPS-T, before and after extraction.

Figure 5 Sorption from 150 mg/L BF solution for xPS and xPS-T, before and after extraction.
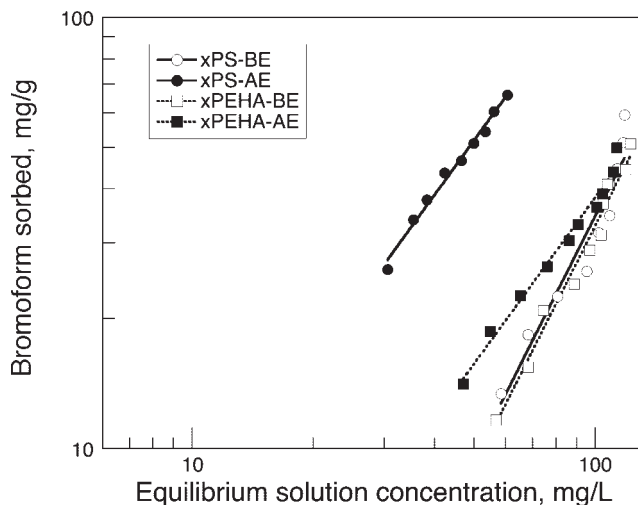
Figure 7 Sorption isotherms for xPS and xPEHA, before and after extraction.

$$\log q_e = \log K + \frac{1}{n} \log C_e \qquad (1)$$

$$q_e = \frac{(C_0 - C_e)V}{m} \qquad (2)$$

where C_e is the equilibrium concentration (mg/L), K is the value of q_e when C_e equals 1 mg/L, n is a constant, q_e is the sorption capacity (mg/g), C_0 is the initial concentration (mg/L), V is the volume of the solution (L), and m is the weight of sorbent (g). The sorption by poly(HIPE) is not the case of adsorption described by Freundlich, but the same form of relationship has been shown to be useful in describing such sorption data.[12,13] The log–log sorption isotherms for xPS and xPEHA, both before and after extraction, are seen in Figure 7. The parameters from a straight line fit to the data, $1/n$, the slope, and K, q_e for $C_e = 1$ mg/L, are listed in Table II.

Sorption increases with the equilibrium concentration for all the poly(HIPE). xPS-BE and xPEHA-BE have similar isotherm parameters, reflecting their similar specific surface areas. The similarity between xPS-BE and xPEHA-BE confirms the conclusions drawn from the sorption rate experiments. $1/n$ decreases in a similar manner for both xPS and xPEHA on extraction, yielding similar values of $1/n$ for xPS-AE and xPEHA-AE. K for xPS-AE is larger than K for xPHEA-AE. This indicates that the sorption capacity is more strongly dependent upon the specific surface area than $1/n$.

The log–log sorption isotherms for xPS and xPS-T, before and after extraction, are seen in Figure 8. The equilibrium sorption behavior of xPS-T-BE is similar to that of xPS and xPEHA. K and $1/n$ for xPS-T-BE are similar to those of xPEHA after extraction, reflecting their similar specific surface areas (Table II). The equi-

librium sorption behavior for xPS-T-AE is more complex than for xPS-T-BE. As seen for xPS, the increase in specific surface area on extraction for xPS-T yields an increase in BF sorption. xPS-T-AE achieved significantly lower equilibrium concentrations for a set of similar initial concentrations. The ability to achieve such low equilibrium concentrations results directly from its significantly higher specific surface area. The sorption behavior of xPS-T-AE can be better described using two straight line fits based on Equation (1) (Fig. 8 and Table II). One fit describes the sorption at lower initial concentrations (lower equilibrium concentrations) and the other fit describes the sorption at higher initial concentrations (higher equilibrium concentrations). The K for xPS-T-AE at lower concentrations is significantly larger than the K from all the other samples. The $1/n$ for xPS-T-AE at lower concentrations is significantly smaller than the $1/n$ from all the other samples. The small $1/n$ indicates that the amount of BF sorbed is relatively constant and independent of concentration.

This more complex sorption behavior seems to indicate that, for xPS-T-AE, there are two sorption mechanisms that can be distinguished. One mechanism is dominant at lower concentrations for large specific surface areas and the other mechanism is dominant both at higher concentrations for large specific surface areas and at all concentrations for small specific surface areas. The relatively constant sorption seen for xPS-T-AE at low concentrations can be associated with a case of adsorption with a constant number of adsorption sites that have all been filled. Once the adsorption sites are filled, no more can be adsorbed, and the amount adsorbed remains constant. In contrast, an absorption mechanism dominates at higher concentrations for larger specific surface areas and at all concentrations for smaller specific surface areas.
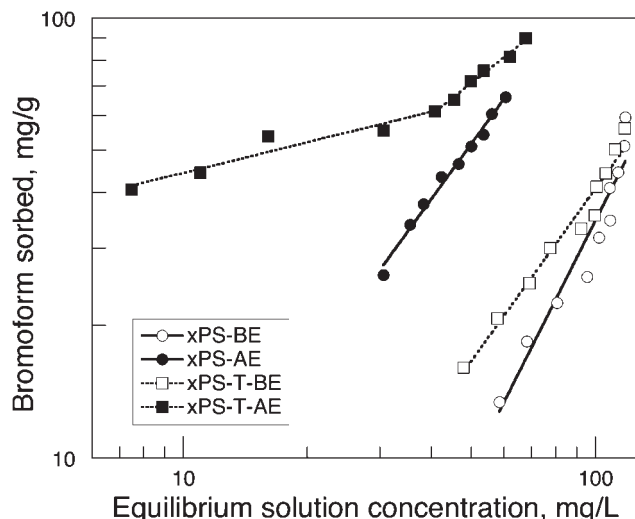

Figure 8 Sorption isotherms for xPS and xPS-T, before and after extraction.

The variations of $1/n$ and K from Equation 1 with the specific surface area for the cases where absorption dominates are described by straight lines in Figures 6(b) and (c), respectively. Data points representing the case where adsorption dominates are included in Figures 6(b) and (c) for comparison. The slopes of the straight line fits in Figure 6 are -0.31 and 1.9 for $1/n$ and K, respectively. As seen from the comparison of xPS-AE and xPEHA-AE, K is more strongly dependent on specific surface area than $1/n$. K, the sorption capacity, reflects the contributions of both adsorption and absorption and is thus more strongly dependent on the specific surface area. $1/n$ represents the dependence of sorption on concentration and, for the cases where absorption dominates, is less dependent on the specific surface area.

CONCLUSIONS

The xPS and xPEHA poly(HIPE) had open-cell structures with cell diameters from 1.5 to 15 μm, intercellular pore diameters from 0.3 to 1.5 μm, and densities of about 0.10 g/cc. The specific surface area of the glassy xPS increased from 7.9 to 28.8 m^2/g, most likely through crazing, following extraction in methanol. The use of a toluene porogen in the xPS reduced the density to 0.05 g/cc and yielded a rough surface with a nanoscale porous structure and a specific surface area of 132 m^2/g. Sorption in the poly(HIPE) is a combination of adsorption and absorption. xPS-BE and xPEHA-BE, with very different molecular structures but with similar specific surface areas, exhibited similar sorption behavior. Extraction produced increases in the xPS and xPS-T sorption plateaus and sorption capacities. For larger specific surface areas, the sorption at low concentrations was relatively independent of concentration. This seems to indicate that sorption is dominated by adsorption with all the sites occupied. For all the other cases, absorption seems to dominate and sorption is more strongly dependent upon concentration. The sorption capacity, which reflects both adsorption and absorption, depends more strongly on the specific surface area than $1/n$, which reflects the dependence of sorption on the concentration.

References

1. Means, E. G.; Krasner, S. W. J Am Water Works Assoc 1993, 85, 68.
2. Andrews, A. R. J.; Ziatkis, A.; Tang, M. T.; Zhang, W.; Shanfield, H. Environ Sci Technol 1993, 27, 1139.
3. Lykins, B. W.; Clark, R. M.; J Environ Eng 1994, 120, 783.
4. Sluzney, A.; Silverstein, M. S.; Kababya, S.; Schmidt A.; Narkis, M. J. Polym Sci, Polym Chem 2001, 39, 8.
5. Sluszny, A.; Silverstein, M. S.; Narkis, N.; Narkis, M. J Appl Polym Sci 2001, 81, 1429.
6. Clark, R. M.; Adams, J. Q. J Environ Eng 1991, 117, 247.
7. Singer, P. C. J Environ Eng 1994, 120, 727.
8. Clark, R. M.; Adams, J. Q.; Lykins, B. W. J Environ Eng 1994, 120, 759.
9. Slejko, F. L. Adsorption Technology; Marcel Dekker: New York, 1985.
10. Shach-Caplan, M.; Narkis, M.; Silverstein, M. S. Polym Adv Technol 2002, 13, 151.
11. Shach-Caplan, M.; Narkis, M.; Silverstein, M. S. Polym Eng Sci 2002, 42, 911.
12. Shach-Caplan, M.; Narkis, M.; Silverstein, M. S. J Polym Eng 2003, 22, 417.
13. Shach-Caplan, M.; Narkis, M.; Silverstein, M. S. Polym Adv Technol 2003, 14, 83.
14. Montgomery, J. M. Water Treatment Principles and Design; Wiley-Interscience: New York, 1985.
15. Kennedy, D. C. US Patent 4042498, 1990.
16. Bohra, P. M; Vaze, A. S.; Pangarkar, V. G. J Chem Technol Biotechnol 1994, 60, 97.
17. Pontius, F. W. Water Quality and Treatment; McGraw-Hill: New York, 1990; 4th ed.
18. Williams, J. M. Langmuir 1988, 4, 44.
19. Williams, J. M.; Wrobleski, D. A. Langmuir 1988, 4, 656.
20. Williams, J. M. Langmuir 1991, 7, 1370.
21. Barby, D.; Haq, Z. Eur Patent 0060138, 1982.
22. Haq, Z. US Patent 4536521, 1985.
23. Hainey, P.; Huxham, I. M.; Rowatt, B.; Sherrington, D. C.; Tetley, L. Macromolecules 1991, 24, 117.
24. Guyot, A. In Synthesis and Structure of Polymer Supports in Syntheses and Separations using Functional Polymers; Sherrington, D. C.; Hodge, P. Eds.; Wiley: New York, 1988.
25. Akay, G.; Bhumgara, Z.; Wakeman, R. J. Trans Inst Chem Eng 1995, 73, 782.
26. Benicewicz, B. C.; Jarvinen, G. D.; Kathios, D. J.; Jorgensen, B. S. J Radioanal Nucl Chem 1998, 235, 31.
27. Wakeman, R. J.; Bhumgara, Z.; Akay, G. Chem Eng J 1998, 70, 133.
28. Tai, H.; Sergienko, A.; Silverstein, M. S. Polym Eng Sci 2001, 41, 1540.
29. Tai, H.; Sergienko, A.; Silverstein, M. S. Polymer 2001, 42, 4473.
30. Sergienko, A. Y.; Tai, H.; Narkis, M.; Silverstein, M. S. J Appl Polym Sci 2002, 84, 2018.
31. Tai, H.W.; Shea, K.; Silverstein, M. PMSE Proc 2002, 86, 235.
32. Plummer, C. J. G.; Donald, A. M. J Mater Sci 1989, 24, 1399.